


Full length article

Inflammation-targeted vesicles for co-delivery of methotrexate and TNF- α siRNA to alleviate collagen-induced arthritisLiang Yang^{a,b,1}, Yongjie Sha^{a,b,1}, Yuansong Wei^c, Lichen Yin^c, Zhiyuan Zhong^{a,b,*}, Fenghua Meng^{a,**} ^a Biomedical Polymers Laboratory, College of Chemistry, Chemical Engineering and Materials Science, and State Key Laboratory of Radiation Medicine and Protection, Soochow University, Suzhou 215123, China^b College of Pharmaceutical Sciences, Soochow University, Suzhou 215123, China^c Institute of Functional Nano & Soft Materials (FUNSOM), Jiangsu Key Laboratory for Carbon-Based Functional Materials & Devices, Collaborative Innovation Center of Suzhou Nano Science & Technology, Soochow University, Suzhou 215123, China

ARTICLE INFO

Keywords:

Rheumatoid arthritis
Combination therapy
RNA interference
Macrophage-targeted delivery
Polymeric vesicles

ABSTRACT

Rheumatoid arthritis (RA) is an autoimmune disease that has a complex pathogenesis and remains tough to treat. The clinical treatments with e.g. methotrexate (MTX) and TNF- α antibodies show fractional responses and lessen the symptoms only to a certain extent. Here, we developed inflammation-targeted vesicles codelivering methotrexate and TNF- α small interfering RNA (siTNF α) (ITV-MT) for effective ablation of collagen-induced arthritis (CIA) in mice. ITV-MT with tetra-mannose ligand and high loading of MTX (17.1 wt%) and siTNF α (9.0 wt%) displayed a small and uniform size (53 nm) and augmented uptake by inflammatory macrophages leading to superior regulation of macrophage phenotype from M1 to M2 *in vitro* compared to monotherapies. The intravenous injection of ITV-MT revealed clearly enhanced accretion in the inflamed joints. Interestingly, ITV-MT effectively repolarized M1 macrophages to M2 type, markedly reduced proinflammatory cytokine levels, and significantly attenuated symptoms including joint swelling, arthritis scores and bone damage in the CIA mouse models, by concurrently downregulating both adenosine and TNF- α pathways. This study highlights inflammation-targeted vesicles codelivering methotrexate and TNF α siRNA as a potential strategy to improved RA treatment.

Statement of significance: Rheumatoid arthritis (RA) is regarded as an incurable disease, often referred to as an "incurable cancer". Current therapies, such as methotrexate (MTX) and anti-TNF α monoclonal antibodies, exhibit limited efficacy and severe adverse effects. The distinct physiochemical properties of MTX and siTNF α hinder their codelivery to RA joints and inflammatory cells. Here, we engineered inflammation-targeted vesicles (ITV-MT) for the codelivery of MTX and siTNF α to enhance therapeutic outcomes. Our findings reveal that ITV-MT significantly improves the drug uptake by macrophages, facilitating repolarization from M1 to M2 phenotypes. In CIA models, ITV-MT effectively downregulated proinflammatory cytokines while upregulating anti-inflammatory cytokines in RA joints, inhibited inflammatory cell infiltration in the synovium and protected against bone erosion. This study highlights that inflammation-targeted co-delivery of small molecular anti-RA agents and RNAi therapeutics may offer a compelling alternative to existing RA treatments, representing a promising strategy for RA treatment.

1. Introduction

Rheumatoid arthritis (RA) is a multifactorial autoimmune disorder

characterized by chronic inflammation, in which inflammatory cells such as macrophages, neutrophils, and lymphocytes play critical roles in its onset and progression [1–3]. The elevated secretion of

* Corresponding author at: Biomedical Polymers Laboratory, College of Chemistry, Chemical Engineering and Materials Science, and State Key Laboratory of Radiation Medicine and Protection, Soochow University, Suzhou 215123, China.

** Corresponding author.

E-mail addresses: zyzhong@suda.edu.cn (Z. Zhong), fhmeng@suda.edu.cn (F. Meng).

¹ These authors contribute equally to this work.

proinflammatory cytokines leads to irreversible damage to the joint synovium and cartilage [4,5]. Both proinflammatory molecules and inflammatory cells significantly influence the severity and underlying mechanisms of RA [6,7]. Current clinical interventions primarily include methotrexate (MTX) and anti-TNF α monoclonal antibodies (infliximab, adalimumab etc.) [8]. As an anti-metabolic drug, MTX modulates the adenosine pathway and inhibits the conversion of folic acid to tetrahydrofolate during DNA synthesis in immune cells. These can lead to the polarization of proinflammatory M1 type macrophage (M1M) into anti-inflammatory M2 type macrophage (M2M) or induce direct cytotoxicity in M1 M in RA lesions at high concentrations, achieving anti-inflammatory effects [9,10]. Anti-TNF α mAb treats RA by blocking TNF- α signaling pathway, which is central to RA pathogenesis [11–13]. Unfortunately, both MTX and anti-TNF α mAb exhibit fractional responses and lessen the symptoms only to a certain extent [14, 15]. Moreover, MTX often shows slow-onset and severe adverse effects upon long-term use [16,17], while anti-TNF α mAb may provoke off-target adverse reactions and lose activity after repeated use [18].

The work from different groups has shown that macrophage-targeted nanodelivery of MTX can enhance its anti-RA effects and safety by improving its pharmacokinetics and uptake in the inflamed joints [19–23]. To solve the problems of anti-TNF α mAb, small interfering RNA targeting TNF α mRNA (siTNF α) has been actively explored [24, 25]. The previous studies showed that siTNF α can downregulate TNF- α level and relieve the inflammatory symptoms of RA joints [26,27]. siTNF α monotherapy leads, however, only to moderate and transient anti-RA effects [11,28,29], which is in part due to inefficient delivery. The combination of siRNA therapeutics with small-molecule drugs like MTX might provide a better treatment for RA by simultaneously targeting two pathways [30–34]. There are, however, rare systems that are able to stably coload and codeliver siRNA therapeutics and water-soluble small drugs as MTX, which have completely different physiochemical properties, to RA joints and inflammatory cells. Severe drug leakage was observed for the nanosystems at pH 7.4 within 12 h

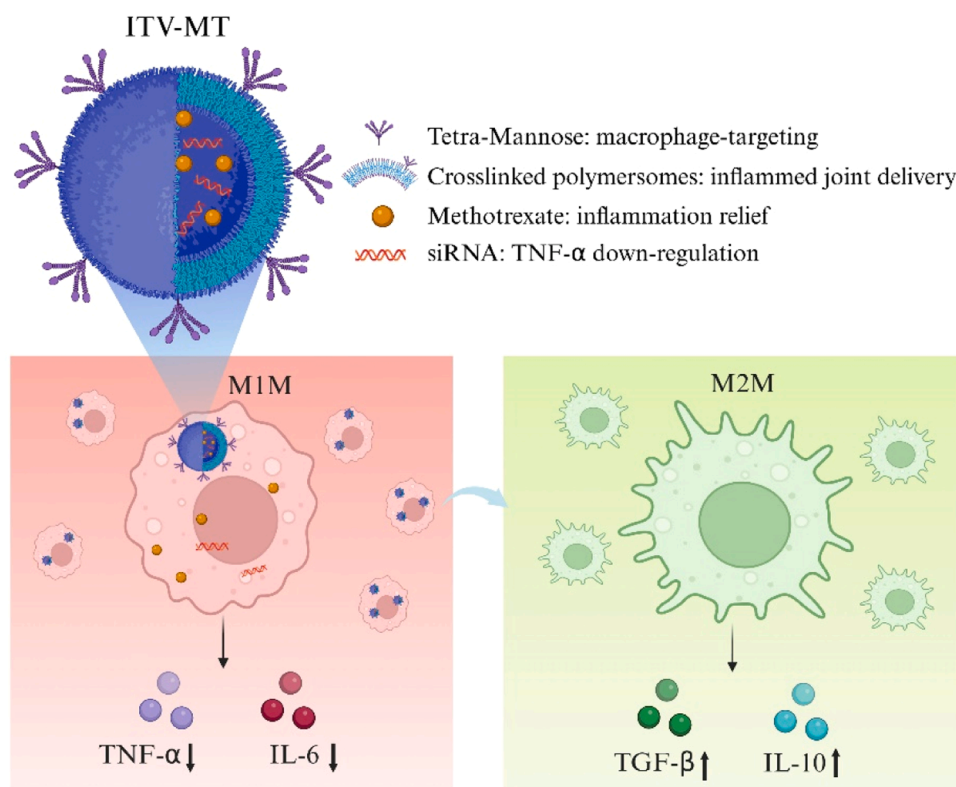
[31,34].

Here, we designed and investigated inflammation-targeted polymeric vesicles for the co-delivery of MTX and siTNF α (ITV-MT) for effective ablation of collagen-induced arthritis (CIA) in mice (Scheme 1). To increase inflammation-targetability, tetra-mannose ligands were equipped at the outer surface of the vesicles to target M1Ms that predominate at RA lesions [35,36]. To efficiently load MTX and siTNF α , chimaeric polymersomes with short polyethylenimine (PEI, 1200 g/mol) in the watery core was employed. Interestingly, ITV-MT showed favorable biophysical features, evident macrophage targetability, and enhanced regulation of the inflammatory microenvironment, leading to marked alleviation of RA symptoms. To our knowledge, this study represents the first report on the targeted co-delivery of small molecular anti-RA agents and RNAi therapeutics to the same inflammatory macrophages at prescribed fixed ratio via chimaeric disulfide-crosslinked polymersomes, providing a potential treatment strategy for RA.

2. Experimental section

2.1. Synthesis and characterization of TM-PEG-P(TMC-DTC)

The tetra-mannose-modified copolymer polyethylene glycol-*b*-poly(trimethylene carbonate-co-dithiolane-trimethylene carbonate) (TM-PEG-P(TMC-DTC)) was synthesized through a two-step process. First, maleimide-functionalized copolymer Mal-PEG-P(TMC-DTC) (MW: 7.5–(15.0–2.0) kg/mol; 158 mg, 0.0064 mmol) in 1 mL of DMSO was added dropwise to a stirred peptide solution of Ac-CGGEGEGE (10 mg, 0.013 mmol) in 100 μ L of DMSO at room temperature for 2 h. The reaction solution was subsequently dialyzed (MWCO: 3500 Da) in 100 mL of DMSO for 16 h (four times dialysate change) and 100 mL of DCM for 8 h (twice dialysate change) before precipitation in 30-fold volume cold ether. This was followed by filtration and vacuum drying at 25 $^{\circ}$ C for 48 h to obtain the Ac-CGGEGEGE modified polymer. Second, the obtained polymer (140 mg, 5.75 μ mol) was dissolved in 1.2 mL of DMSO and



Scheme 1. Schematic illustration of tetra-mannose containing ligands functionalized polymersomes (ITV-MT) for the codelivery of MTX and siTNF α to CD206-overexpressing macrophages in the inflammatory joints of CIA mice.

mixed with N-hydroxysuccinimide (NHS, 5.3 mg, 0.046 mmol) and dicyclohexylcarbodiimide (DCC, 9.5 mg, 0.046 mmol) at 25 °C to activate the carboxylate groups for 12 h. The mixture was then added dropwise to triethylamine-desalted mannose (10.2 mg, 0.046 mmol) under stirring. After 24 h, TM-PEG-P(TMC-DTC) was purified and recovered using the same procedure as above involving dialysis, precipitation and vacuum-drying. ^1H NMR spectrum ($\text{DMSO}-d_6$, 600 MHz, ppm) of TM-PEG-P(TMC-DTC): δ 1.94 (e, $-\text{OCOCH}_2\text{CH}_2\text{CH}_2\text{CO}-$), 3.07 (f, $-\text{C}(\text{CH}_2\text{SSCH}_2)\text{C}-$), 3.51 (b, $-\text{CH}_2\text{CH}_2\text{O}-$), 4.13 (c, $-\text{OCOCH}_2\text{CH}_2\text{CH}_2\text{O}-$), 4.14 (d, $-\text{OCOCH}_2(\text{CH}_2\text{SSCH}_2)\text{CH}_2\text{O}-$) and δ 4.64–4.90 (mannose).

2.2. Preparation of inflammation-targeted vesicles codelivering MTX and siTNF α (ITV-MT)

To prepare ITV-MT, TM-PEG-P(TMC-DTC) and PEG-P(TMC-DTC)-PEI (MW: 5-(14.9–2.2)–1.2 kg/mol) were mixed at a mass ratio of 1:9 in DMF (10 mg/mL, 100 μL), and added into 900 μL of HEPES buffer (5 mM, pH 6.0) containing MTX (300 μg) and siTNF α (0.1 mg) under mild magnetic stirring (280 rpm) for 1 h. The formed polymersomes were dialyzed (MWCO: 3500 Da) in the buffer for 4 h and in phosphate buffer (PB, 5 mM, pH 7.4) for 2 h, with dialysate changes every hour. Single drug-loaded polymersomes, ITV-M and ITV-T, were prepared in the same way but with only one drug (MTX or siTNF α) added. V-MT was prepared without addition of TM-PEG-P(TMC-DTC). Drug loading efficiency (DLE) and drug loading content (DLC) of MTX were measured by UV spectrometer (298 nm), and those data of siTNF α were determined by NanoDrop spectrometer. To determine the loading contents of MTX and siRNA in coloaded polymersomes, ITV-MT (containing 3 % Cy5-siRNA as a probe) was measured using UV–vis spectroscopy at ex. 298 and 647 nm, respectively, and DLCs were calculated based standard curves of MTX or Cy5 from known concentrations. The colloidal stability of ITV-MT during storage and in the presence 10 % serum as well as drug leakage during storage were studied.

2.3. In vitro repolarization of macrophages

RAW 264.7 cells were seeded in 12-well plates (5×10^5 /well) and treated with ITV-M, ITV-T, or ITV-MT (MTX: 20 $\mu\text{g}/\text{mL}$, siTNF α : 100 nM, $n = 3$) for 24 h. The medium was supplemented with LPS (100 ng/mL) and incubated for an additional 4 h. The concentrations of TNF- α , IL-1 β , IL-6 and IL-10 in the medium were measured using ELISA kits.

Bone marrow derived macrophages (BMDMs) were cultured in 12-well plates (1×10^6 /well), and treated with PBS, ITV-M, ITV-T, or ITV-MT (MTX: 20 $\mu\text{g}/\text{mL}$, siTNF α : 100 nM) for 24 h. The medium was then supplemented with LPS (100 ng/mL) and IFN- γ (20 ng/mL) and incubated for an additional 4 h. The concentrations of TNF- α and IL-1 β in the medium were measured using ELISA kits.

2.4. In vivo and ex vivo fluorescence images of CIA mice

All animal experiments were approved by the Animal Care and Use Committee of Soochow University (P. R. China) and all protocols for the animal studies conformed to the Guide for the Care and Use of Laboratory Animals. The collagen-induced arthritis (CIA) mouse model was established on male DBA/1 mice (6–8 weeks, 16–18 g) as previously reported [37]. An emulsion of bovine type II collagen and Freund's Complete Adjuvant was intradermally injected into the tail base of the mice for initial immunization. After 21 days, these mice were boosted with an emulsion of bovine type II collagen and Freund's incomplete adjuvant. Disease progression was monitored by measuring hind paw thickness and the arthritis score, with each limb scored on a scale of 0–4 (maximum score: 16).

In vivo live imaging was performed when the four paws became swollen. CIA mice were intravenously injected with 200 μL of Cy5-labeled V-MT or ITV-MT (Cy5: 0.3 $\mu\text{g}/\text{mouse}$, siTNF α : 0.5 mg/kg (mpk), MTX: 4 mpk) via tail veins. At predetermined time points, the

mice were scanned using an IVIS imaging system to study the bio-distribution of the nanodrugs ($n = 3$). At 24 h post-injection, the mice were sacrificed, and their hind legs were collected for *ex vivo* imaging and semiquantitative analysis.

2.5. In vivo therapeutic efficacy of ITV-MT in RA mice

When the arthritis score reached 2–3, the CIA mice were randomly divided into five groups ($n = 8$): PBS, a mixture of free MTX and siTNF α (siTNF α : 1 mpk, MTX: 4 mpk), ITV-M (MTX: 4 mpk), ITV-T (siTNF α : 1 mpk), or ITV-MT (siTNF α : 0.5 mpk, MTX: 4 mpk). Each group received 200 μL i.v. injection every 4 days for a total four injections, with the first injection day designated as day 0. Arthritis score and paw thickness were evaluated every two days. On day 16, the fore and hind limbs of the mice were photographed. Five mice of each group were then sacrificed, and blood samples were collected to measure cytokine concentrations using ELISA kits ($n = 5$). Ankle tissues were collected and divided into two parts for cytokines and mRNA analysis. Cytokine concentrations were measured using ELISA kits and normalized to pg/mg protein, with protein content quantified using BCA assays ($n = 5$). For the second part of ankle tissue, total RNA was extracted from the synovium and cartilage using TRIzol extract, purified, dried and analyzed via real-time PCR (RT–PCR) for mRNA expression of TNF- α and IL-6 genes, normalized to the PBS group ($n = 5$). The main organs of one mouse from each group were sliced and stained with H&E. The ankle tissue of hind limb of one mouse was used for western blotting to determine TNF- α expression.

Additionally, on day 16, three mice from each group were sacrificed and six hind leg bones were collected for histological analysis. Three hind leg bones including knee joints and ankle joints were fixed, decalcified, and sliced for staining with TNF- α antibody, H&E, or safranin O/fast green ($n = 3$). Images were observed via light microscopy, and pathological scores for inflammation, pannus and bone erosion were determined using a reported scoring method [38] (Table S1). The remaining three hind leg bones were fixed for one week and scanned with a small animal micro CT (μCT) instrument for imaging of the tibia and femur. The data were analyzed and 3D images were reconstructed using NRecon software ($n = 3$).

2.6. Statistical analysis

Data are presented as the mean \pm standard deviation (SD) unless otherwise stated. Significant differences among groups were determined by one-way ANOVA with Tukey's multiple comparison test using GraphPad Prism 9 software. * $p < 0.05$ indicated a significant difference, and ** $p < 0.01$, *** $p < 0.001$, **** $p < 0.0001$ indicated highly significant differences.

3. Results and discussion

3.1. Preparation of ITV-MT

Inflammation-targeted vesicles for the codelivery of MTX and siTNF α (ITV-MT) were facilely produced from the co-self-assembly of 10 % TM-PEG-P(TMC-DTC) ($M_n = 7.5$ –(15.0–2.0) kg/mol) and 90 % PEG-P(TMC-DTC)-PEI triblock copolymer ($M_n = 5.0$ –(14.9–2.2)–1.2 kg/mol) in the presence of MTX and siTNF α (Fig. 1A). TM-PEG-P(TMC-DTC) was obtained by conjugating Mal-PEG-P(TMC-DTC) with Ac-CGGEAGE peptide, followed by the coupling of mannose via an amidation reaction (Fig. S1). ^1H NMR spectrum of TM-PEG-P(TMC-DTC) displayed characteristic peaks of mannose moieties at δ 4.64–4.90 with a TM functionality exceeding 90 % as determined by end-group analysis (Fig. S2). The resulting polymersomes, self-assembled from PEG-P(TMC-DTC)-PEI triblock copolymer, possessed an asymmetric membrane structure. The inner shell, composed of the short hydrophilic PEI, faced the cavity allowing for complexation with MTX and siTNF α through electrostatic interactions. The long PEG outer shell ensured extended circulation

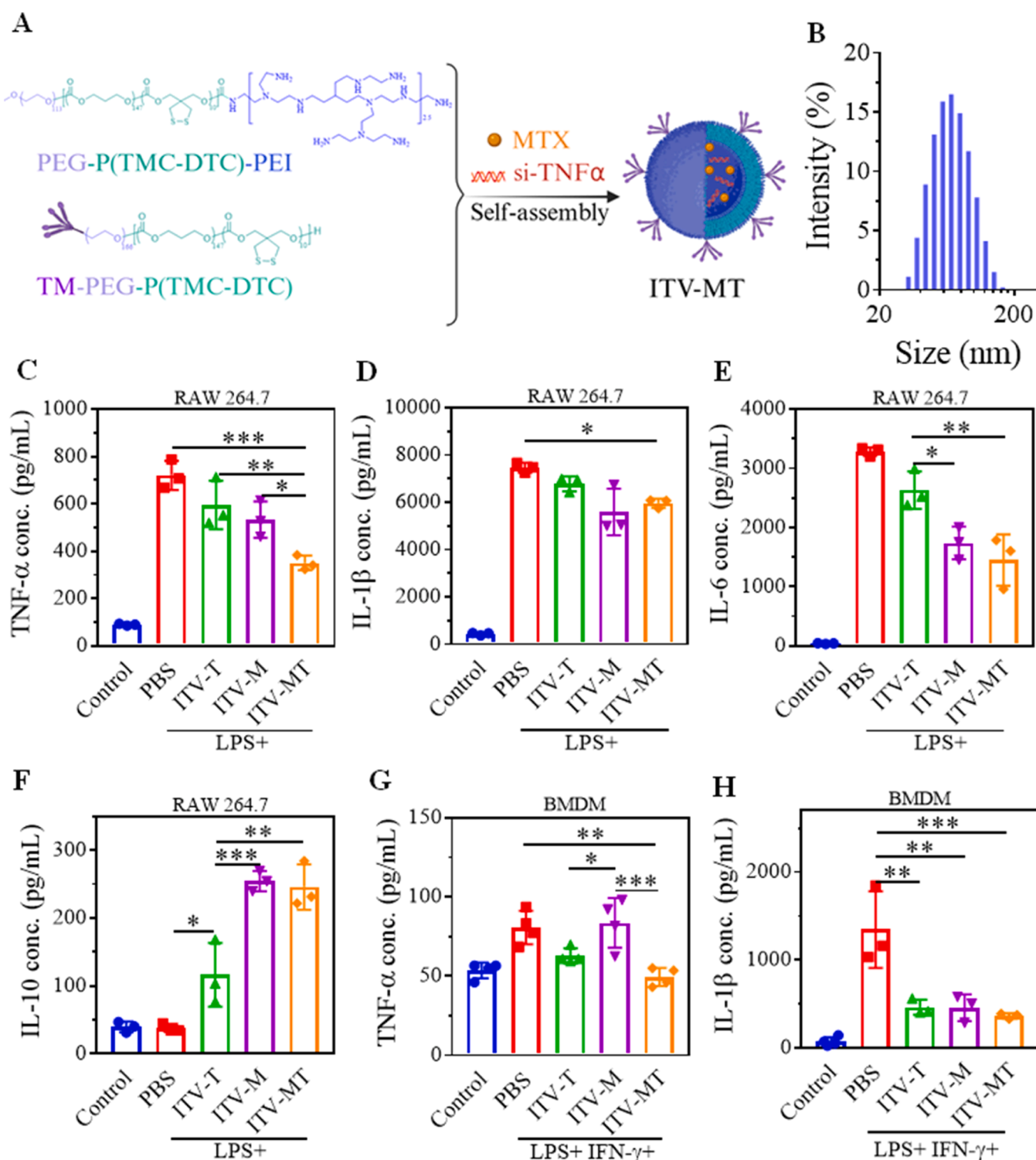


Fig. 1. Size distribution and in vitro repolarization of ITV-MT. (A) Schematic illustration of the preparation of ITV-MT and (B) its size distribution profile. Concentrations of (C) TNF- α , (D) IL-1 β , (E) IL-6, and (F) IL-10 secreted by LPS-stimulated RAW 264.7 cells after 24 h of incubation with ITV-T, ITV-M and ITV-MT. Concentrations of (G) TNF- α and (H) IL-1 β secreted by LPS- and IFN- γ -stimulated BMDMs. PBS, ITV-T, and ITV-M were used as controls (MTX: 20 μ g/mL, siTNF α : 100 nM, $n = 3$). For Fig. 1G, $n = 4$.

time, while the disulfide-crosslinked hydrophobic membrane made of P (TMC-DTC) served as a barrier, effectively separating the inner compartment from the external environment [39]. This structural design enabled high and stable loading of both highly water-soluble MTX and siRNA, which is generally challenging to achieve. The surface density of TM on the vesicle could be tailored by varying the copolymer

composition. Of note, ITV-MT displayed a high loading for both MTX and siTNF α (Table S2) with uniform hydrodynamic sizes. Typically, ITV-MT was obtained with a TM density of 10 %, an MTX loading content of 17.1 wt% and a siTNF α loading content of 9.0 wt% (Fig. 1B), and they appeared as small nanoparticles with a spherical vesicular structure as seen from scanning electron microscope (SEM) and

transmission electron microscope (TEM) images, respectively (Fig. S3A). Non-targeted controls (V-MT, V-M and V-T), single-drug counterparts (ITV-M and ITV-T) were prepared similarly. Dynamic light scattering (DLS) measurements indicated that all formulations had similar and small size (49–53 nm) and low polydispersity (PDI: 0.08–0.15) (Fig. S3B), indicating a minimal influence of payload and surface mannose. Interestingly, the spontaneously formed disulfide-crosslinks in the hydrophobic P(TMC-DTC) membrane during the polymersome workup served as a dense barrier to mitigate leakage of MTX and siRNA, in addition to the effects of electrostatic interactions. ITV-MT exhibited good stability in 10 % FBS or during storage at 4 °C with minor drug leakage observed over a period of at least four weeks (Fig. S3C,D,E). The encapsulated MTX and siTNF α may be triggered to release in cytoplasm-mimicking reductive conditions through cleavage of disulfide bonds. This disulfide-crosslinking mechanism effectively prevents drug leakage during circulation and enhances the drug release efficacy within the cytoplasm. Furthermore, ITV-MT, V-MT and monotherapies, with MTX conc. of 200 μ g/mL and siTNF α conc. of 100 μ g/mL, which were used for subsequent *in vivo* investigations, did not show hemolysis (Fig. S3F), implying their safety as intravenous formulation.

3.2. Anti-inflammatory effect of ITV-MT

We evaluated the cellular uptake and anti-inflammatory effects of ITV-MT *in vitro* inflammation models using M1M-dominant macrophages, specifically RAW 264.7 cells or BMDMs stimulated with lipopolysaccharide (LPS). To investigate the influence of tetra-mannose (TM) density on the uptake of ITV-MT by LPS-stimulated BMDMs, we employed Cy5-labeled polymersomes. Flow cytometry results demonstrated that ITV-MT containing 10 % TM exhibited the highest uptake compared to formulations with 0 %, 5 % and 20 % TM densities (Fig. S4A). Notably, the uptake at 10 % TM density was 1.6-fold greater than that observed with formulations containing either 10 % or 40 % mannose (Fig. S4B). This increased uptake is attributed to the multivalent binding of tetra-mannose to mannose receptors on macrophages. Consequently, ITV-MT with 10 % TM density was selected for subsequent studies.

The levels of the proinflammatory cytokines TNF- α , IL-1 β , and IL-6 and the anti-inflammatory cytokine IL-10 were measured. ELISA results demonstrated a reduction in TNF- α concentration in both ITV-M and ITV-T groups compared to the PBS group, and TNF- α was further significantly reduced by ITV-MT treatment (Fig. 1C). Similarly, IL-6 and IL-1 β concentrations were notably lower in the ITV-MT group than in other groups (Fig. 1D&E). Moreover, IL-10 levels were significantly higher in the ITV-MT group compared to the PBS (***) and ITV-T (**) groups (Fig. 1F). BMDMs treated with ITV-MT followed similar trends and secreted lower levels of TNF- α and IL-1 β than those from the ITV-M and ITV-T groups, and significantly lower levels than the PBS group (Fig. 1G&H). It is known that M1Ms secrete proinflammatory cytokines (TNF- α , IL-1 β and IL-6 are key markers), while M2Ms secrete anti-inflammatory cytokines (IL-10 is a key marker). These results suggest that ITV-MT effectively reduces M1Ms and increases M2Ms, demonstrating a superior ability to regulate macrophage phenotype from M1Ms to M2Ms.

3.3. Targeting of ITV-MT to RA joints

To investigate the inflammation-targetability of ITV-MT in collagen-induced arthritis (CIA) mice, the biodistribution and its accumulation in RA inflammatory joints were studied using Cy5-labeled ITV-MT or V-MT for tracking. *In vivo* imaging demonstrated a significant increase in Cy5 fluorescence in the limbs for both groups at 2 h post intravenous (i.v.) injection, attributed to the enhanced vascular permeability and retention (ELVIS) effect at the site of inflammation. Remarkably, from 2 to 8 h, the accumulation of ITV-MT in the RA joints progressively increased, maintaining a high level from 12 to 24 h, in contrast to the lower

accumulation of V-MT (Fig. 2A). In particular, Cy5 intensity in the joints of the ITV-MT group was 3.2-fold higher than that of the V-MT group at 24 h (**). *Ex vivo* fluorescence images of the limbs at 24 h confirmed an enhanced enrichment of Cy5 in the inflammatory feet and ankle joints of ITV-MT-treated mice, with fluorescence intensity twice that of the V-MT group (*) (Fig. 2B). In particular, radiant efficiencies of inflamed ankle joints of hind legs (A) in ITV-MT group were significantly higher than those in healthy muscles (M, **) of the same mice, while such difference was not observed for V-MT group (Fig. 2B). These results confirmed the macrophage-targeting effect of the TM cluster due to the multivalent binding to CD206 on macrophages. It is reported that polysaccharides with branched structures exhibit improved binding affinity for CD206 compared to those with linear structures [40,41] and mono mannose [42,43], attributed to the strong binding of long-chain branched sugars to the CRD4-8 on CD206 [35]. The active targeting and long retention of ITV-MT in the inflammatory joints of CIA mice, providing a basis for drug release at inflammatory sites and anti-inflammatory effects for anti-CIA treatment.

3.4. Therapeutic efficacy of ITV-MT in ZIA mice

The therapeutic effect of ITV-MT was preliminarily evaluated using a zymosan A-induced RA (ZIA) mouse model with a single i.v. injection (MTX: 4 mg/kg, siTNF α : 1 mg/kg). ZIA model generally serves as a primary model for innate immunity in RA, simulating the role of macrophages in activating inflammation and damaging articular cartilage during the early stages of RA, thus suitable for preliminary and rapid screening of anti-inflammatory effects. Changes in body weight, knee diameter and circumference, and cytokine concentrations in the plasma were monitored over time (Fig. 3A). With no significant changes in body weight observed all groups (Fig. 3B), ITV-MT group at half the dose of siTNF α showed a substantial reduction in leg swelling and knee diameter/circumference compared to the two monotherapy groups (Fig. 3C and D). Moreover, the plasma concentration of IL-6 was greatly lower in the ITV-MT group than in the two monotherapy groups (**) on day 3, despite no significant difference on days 1 and 2 (Fig. 3E). These results validate that a single injection of ITV-MT could downregulate proinflammatory cytokines expression in ZIA mice, demonstrating synergistic effects. This finding is consistent with reports on the benefit of combining MTX with TNF inhibitors in seropositive RA patients [12].

3.5. Therapeutic efficacy of ITV-MT in CIA mice

The anti-RA efficacy of ITV-MT was further systematically evaluated in CIA mouse model, which is characterized by an autoimmune response against type II collagen in articular cartilage with prolonged joint inflammation and tissue damage. CIA models built in DBA/1J mice contain MHC II H-2^q genotype that increases the susceptibility to type II collagen, closely resembling the pathogenesis and immunological situation in RA patients associated with specific HLA-DRB1 alleles that predispose them to autoantigen-related disease mechanisms [44–46]. These features distinguish it from the CIA and adjuvant-induced arthritis (AIA) rat models.

At arthritis scores of 2–3 (designated as day 0), the mice were i.v. administered with ITV-MT (MTX: 4 mg/kg, siTNF α : 0.5 mg/kg, Fig. 4A). Changes in the arthritis score, paw thickness, cytokine secretion, and bone status were assessed. Results showed that the arthritis scores and paw thickness in the free MTX+siRNA group were only slightly lower than those in the PBS group, due to the short circulation time and easy degradation of naked siRNA *in vivo* (Fig. 4B–D). Treatments with ITV-M and ITV-T slightly improved the arthritis scores and reduced paw swelling. In contrast, ITV-MT significantly decreased the arthritis score and swelling (Fig. 4B), effectively preventing RA progression. On day 16, paw thickness was reduced to a level comparable to that of healthy mice (Fig. 4C, D). Images of the hind and forelimbs showing no visible redness or swelling of the paw pads, similar as healthy mice, confirmed

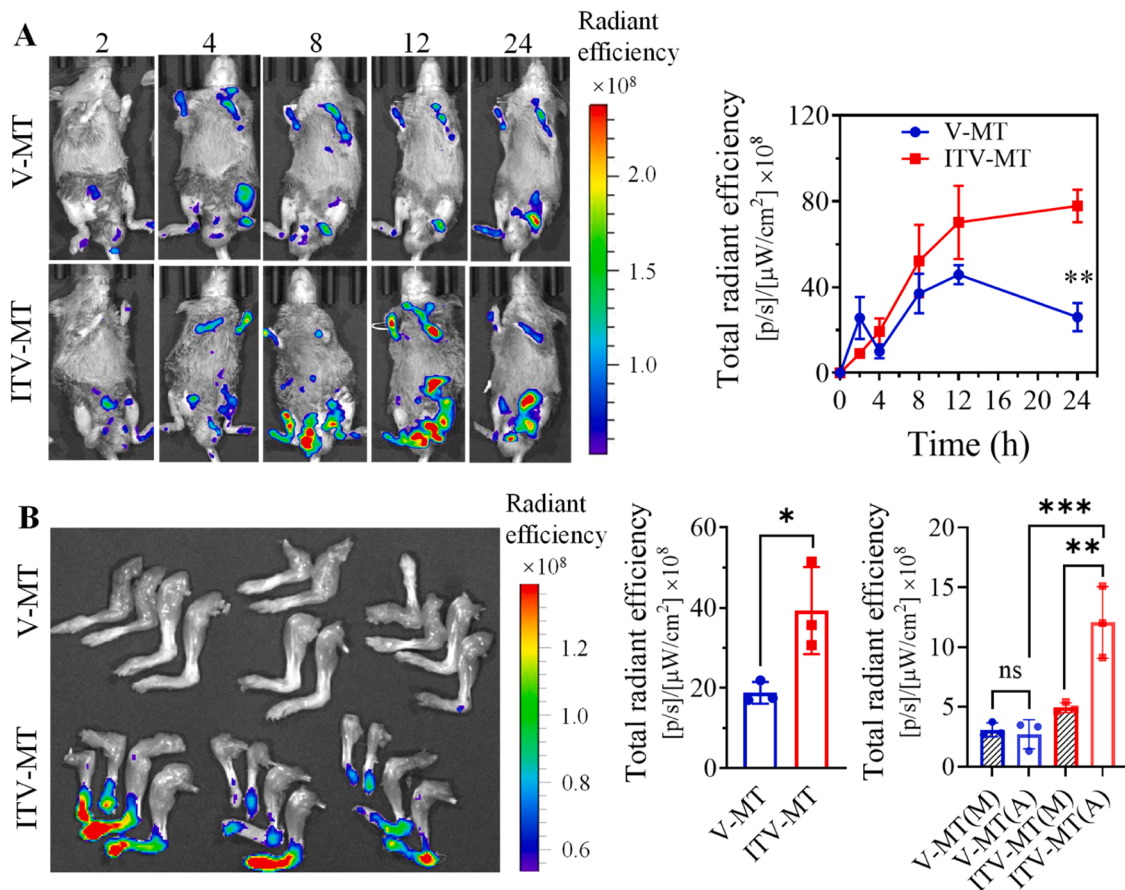


Fig. 2. In vivo biodistribution of Cy5-labeled V-MT and ITV-MT (Cy5: 0.3 $\mu\text{g}/\text{mouse}$, $n = 3$). (A) In vivo imaging and semiquantification of the mice. (B) Ex vivo images and semiquantification of total radiant efficiency of four limbs as well as radiant efficiency of inflammatory ankles of hind legs (A) and healthy muscles (M) at 24 h post-injection.

the anti-inflammatory capacity of ITV-MT (Fig. 4E).

Hematoxylin and eosin (H&E) staining revealed no significant toxicity to the major organs in treated mice compared to the PBS-treated RA mice (Fig. S5), indicating favorable biosafety profiles for ITV-MT. It is important to note that off-target effects of siTNF α can lead to reduced efficacy and inaccurate gene knockout, potentially resulting in systemic toxicity. The targeted delivery capability of ITV-MT for M1M substantially mitigates off-target effects, minimizing damage to normal stromal cells. Studies have shown that MTX synergizes with TNF- α antagonists in seropositive RA patients [12,47], while siTNF α -loaded lipid nanoparticles could not reduce hind leg paw thickness in a CIA mouse model at high doses (2 mg siRNA/kg) [27]. The better anti-RA effect of ITV-MT signifies the importance of siTNF α and MTX co-delivery at a prescribed ratio.

3.6. Immunological analyses of inflammatory joints of CIA mice

Immunological analyses of the microenvironment of CIA mice were conducted on day 16. The results confirm the considerably elevated TNF- α and IL-6 in serum and RA joint for the PBS group (model group) compared to healthy mice. On day 16, ITV-MT treatment significantly reduced the serum levels of IL-6 while hardly influenced serum levels of TNF- α , possibly due to very low concentrations close to the detection limit of ELISA kit (Fig. 5A and B). To further examine the anti-inflammatory ability of ITV-MT in situ, the synovium and cartilage of the limbs of CIA mice on day 16 were homogenized for ELISA analysis of cytokines. The results showed that compared to the PBS group, ITV-MT group exhibited significantly lower concentrations of TNF- α , IL-6 and IL-1 β (Fig. 5C-E), and higher IL-10 levels and IL-10/IL-6 ratio (Fig. 5F-G),

closely resembling the levels in the healthy group. The discrepancy in TNF- α trend in serum and RA joint by ITV-MT treatment may indicate the migration of TNF- α , as an early marker, from peripheral blood to the inflammatory sites in CIA model, causing tissue damage. Additionally, compared with two monotherapies, ITV-MT treatment strongly suppressed expression of TNF- α mRNA and IL-6 mRNA in RA joints, as detected by RT-PCR, effectively regulating the inflammatory microenvironment of RA (Fig. 5G, H). Western blotting revealed that TNF- α protein levels in the RA joint tissues followed a trend similar to that of the ELISA and RT-PCR results (Fig. S6). These findings confirm that ITV-MT is more effective at reducing the expression of proinflammatory genes and proteins and remodeling the immune microenvironment in RA joints than single-drug counterparts.

3.7. Joint tissue analyses of CIA mice

Bone injury or destruction is a common occurrence during RA pathogenesis. To evaluate the therapeutic effects of ITV-MT on the joint bone and cartilage tissue of CIA mice, knee and ankle sections were stained with H&E, safranin O fast green (SO-FG), or subjected to TNF- α immunohistochemical (IHC) staining. Analysis of bone and cartilage destruction, immune cell infiltration, and TNF- α distribution was performed (Fig. 6A). H&E-staining revealed severe synovium destruction and presence of a large number of infiltrating immune cells (orange arrows point to severe inflammation areas) in the knee and ankle joints in the PBS group. Inflammation in these joints and damage to articular cartilage were reduced in the monotherapies and free drug groups. In contrast, the ITV-MT group exhibited nearly no inflammation, a smooth synovium, and a complete ankle joint structure resembling that of

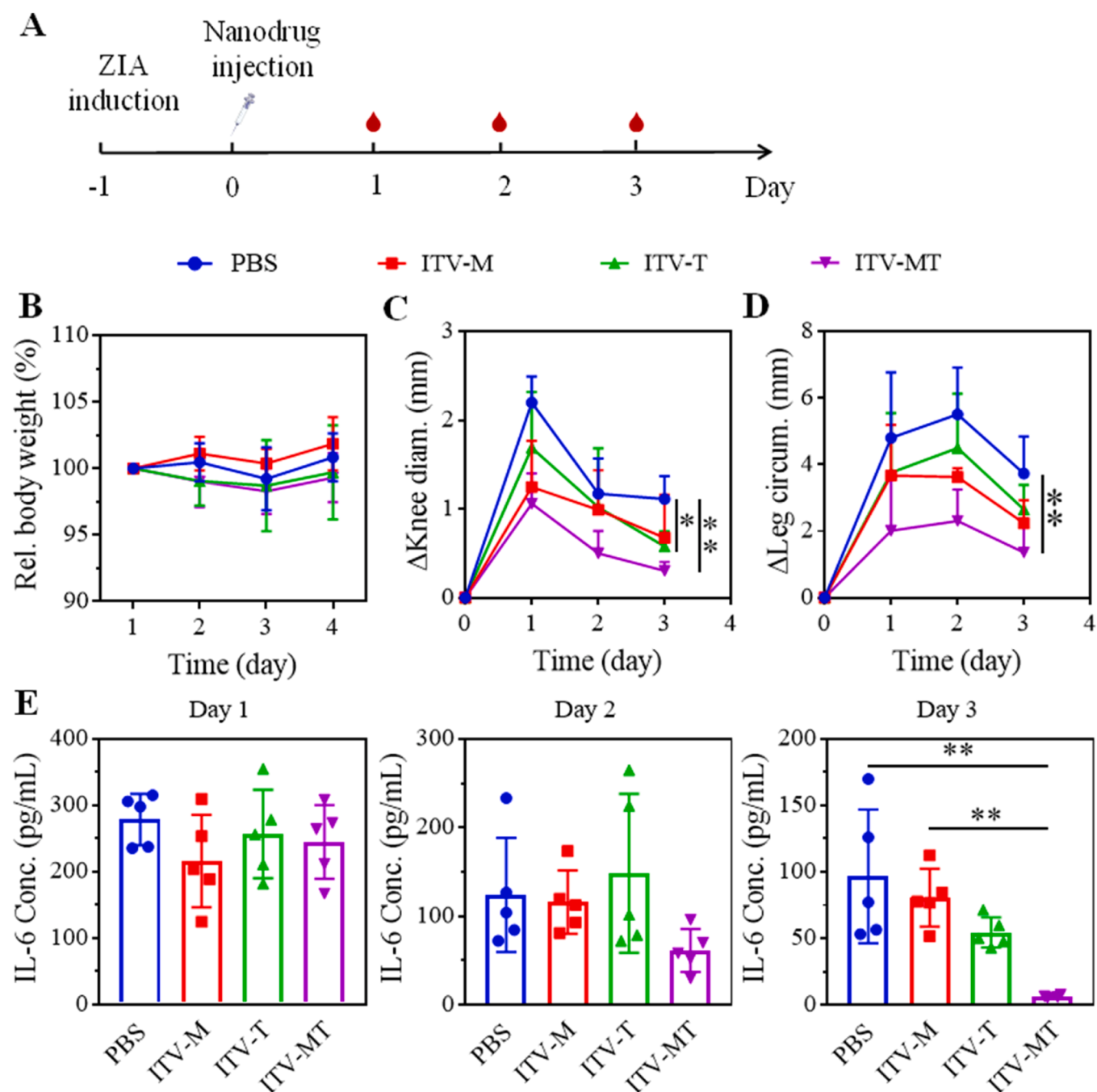


Fig. 3. Anti-RA effects of ITV-M (4 mg/kg), ITV-T (siTNF α : 1 mg/kg) and ITV-MT (MTX: 4 mg/kg, siTNF α : 0.5 mg/kg) on ZIA mice ($n = 5$). (A) Experimental schedule. (B) Relative body weight of the mice. Changes in the knee (C) diameter and (D) circumference of the RA joints. (E) Plasma IL-6 concentrations on days 1, 2 and 3 ($n = 5$).

healthy mice. Moreover, TNF- α IHC staining of ITV-MT group revealed very small TNF- α -positive regions (similar to those in the healthy group) and a reduction in immune cell infiltration within the synovium, in contrast to the significant joint damage and large TNF- α -positive areas in the synovium (white arrows point to high TNF- α positive areas) of the free drug, ITV-M and ITV-T groups (Fig. 6A). Semi-quantitative analyses of synovial inflammation arthritis score and pannus score of ITV-MT group decreased from 3 to 0.5, indicating the great capacity to reduce inflammation and new pannus formation (Fig. 6B).

SO-FG stained images showed that compared to the bones of PBS, free drugs and ITV-T group exhibiting severe loss of bone integrity and cartilage (red arrows point to damaged cartilage), the bone structure in the ITV-M group remained intact despite significant loss of

glycosaminoglycans in the cartilage (Fig. 6A), consistent with reports of some protective effects of MTX on RA bone tissue [48]. Remarkably, the bone tissue of the ITV-MT group was well protected, and the cartilage had integrity and was essentially the same as that of the healthy group, yielding the lowest bone erosion score (Fig. 6B).

Furthermore, the protective effect of ITV-MT against bone erosion in the periarticular region and systemic bone loss was analyzed via micro-computed tomography (μ CT) (Fig. 7). 3D reconstructed μ CT images of the cross-sections of tibias and femurs revealed severe damage in the PBS group, while ITV-MT treatment significantly alleviated bone erosion (Fig. 7A, C). The bone structure parameters supported this observation, showing significantly increased bone volume fraction (BV/TV), trabecular thickness (Tb.Th), trabecular number (Tb.N) and bone mineral

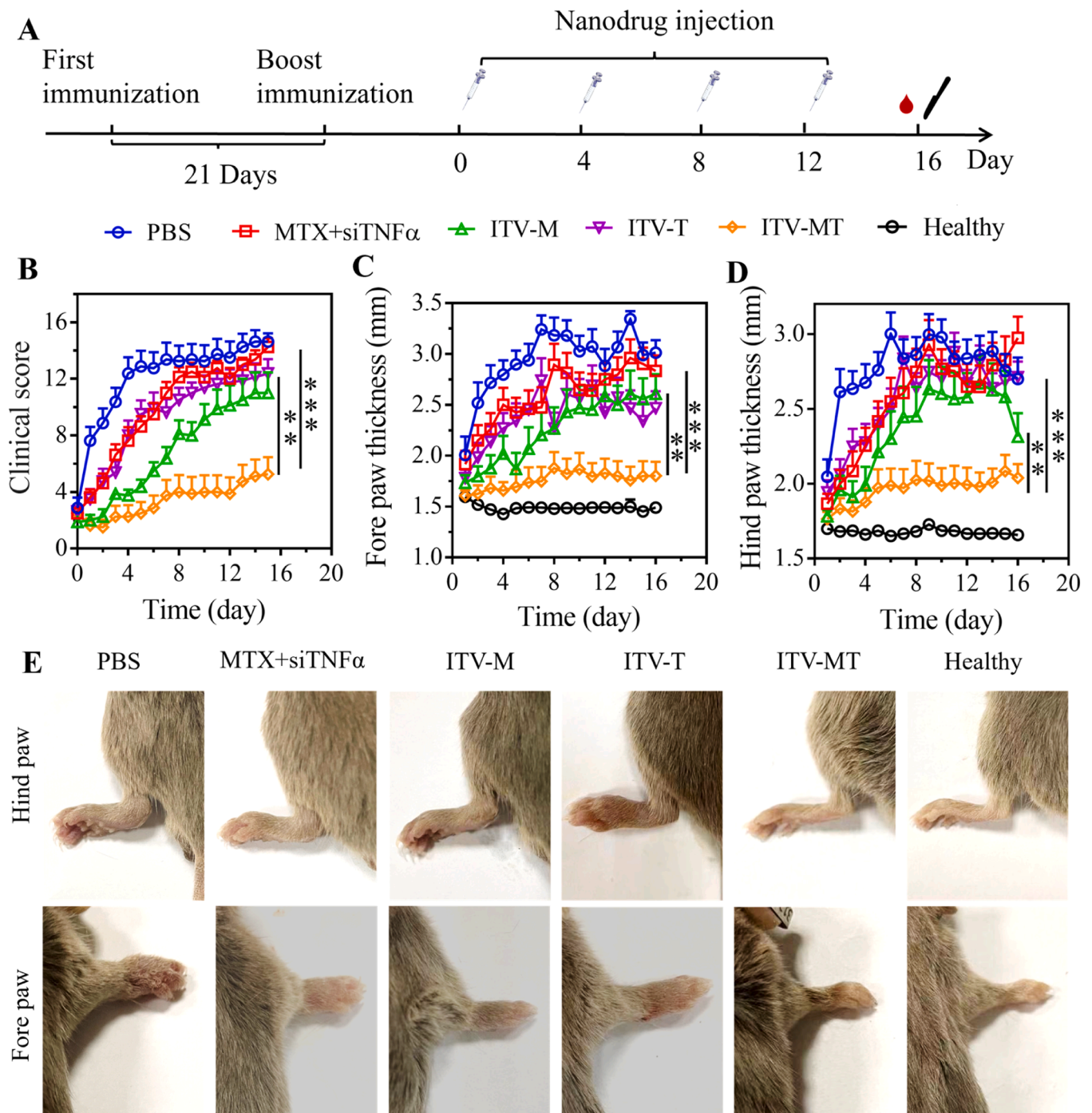


Fig. 4. In vivo anti-CIA efficacy of ITV-M (4 mpk), ITV-T (siTNF α : 1 mpk), free MTX+siTNF α and ITV-MT (MTX: 4 mpk, siTNF α : 0.5 mpk, $n = 8$). (A) Experimental schedule. (B) Arthritis scores, (C) forepaw thickness and (D) hind paw thickness of the mice and the corresponding statistical analysis on day 16. The data are presented as the mean \pm standard error of the mean (SEM). (E) Photographs of representative fore and hind limbs of the mice on day 16.

density (BMD), as well as decreased trabecular separation (Tb.Sp) and bone surface/volume ratio (BS/BV) in both tibias and femurs (Fig. 7B, D). Based on the significant reduction in pro-inflammatory immune cell infiltration and the associated damage to cartilages and bones within RA joints, it is reasonable to anticipate that ITV-MT therapy has the potential to prevent inflammatory relapse, preserving joint health and function over the long term.

Despite the promising results of ITV-MT, complete remission in CIA mice has not yet been achieved. Future investigations should address several critical aspects: (1) The complex interplay of various immune cell types and the intricate immune microenvironment in RA lesions [49,

50] necessitates the development of innovative therapies that integrate multiple drugs to effectively target the diverse pathogenic cell populations involved. (2) Given the multifactorial nature of RA, combination therapies should rationally balance anti-inflammatory responses with tissue repair needs at different disease stages. This requires comprehensive nanomedicine designs that enable precise spatiotemporal coordination in drug delivery, allowing for the release of drugs tailored to specific cell types or tissues at optimal times. (3) While CIA murine models have been instrumental in studying RA, their translational relevance to human patients may be limited. Utilizing human tumor necrosis factor transgenic (hTNFtg) mice [51] may provide a

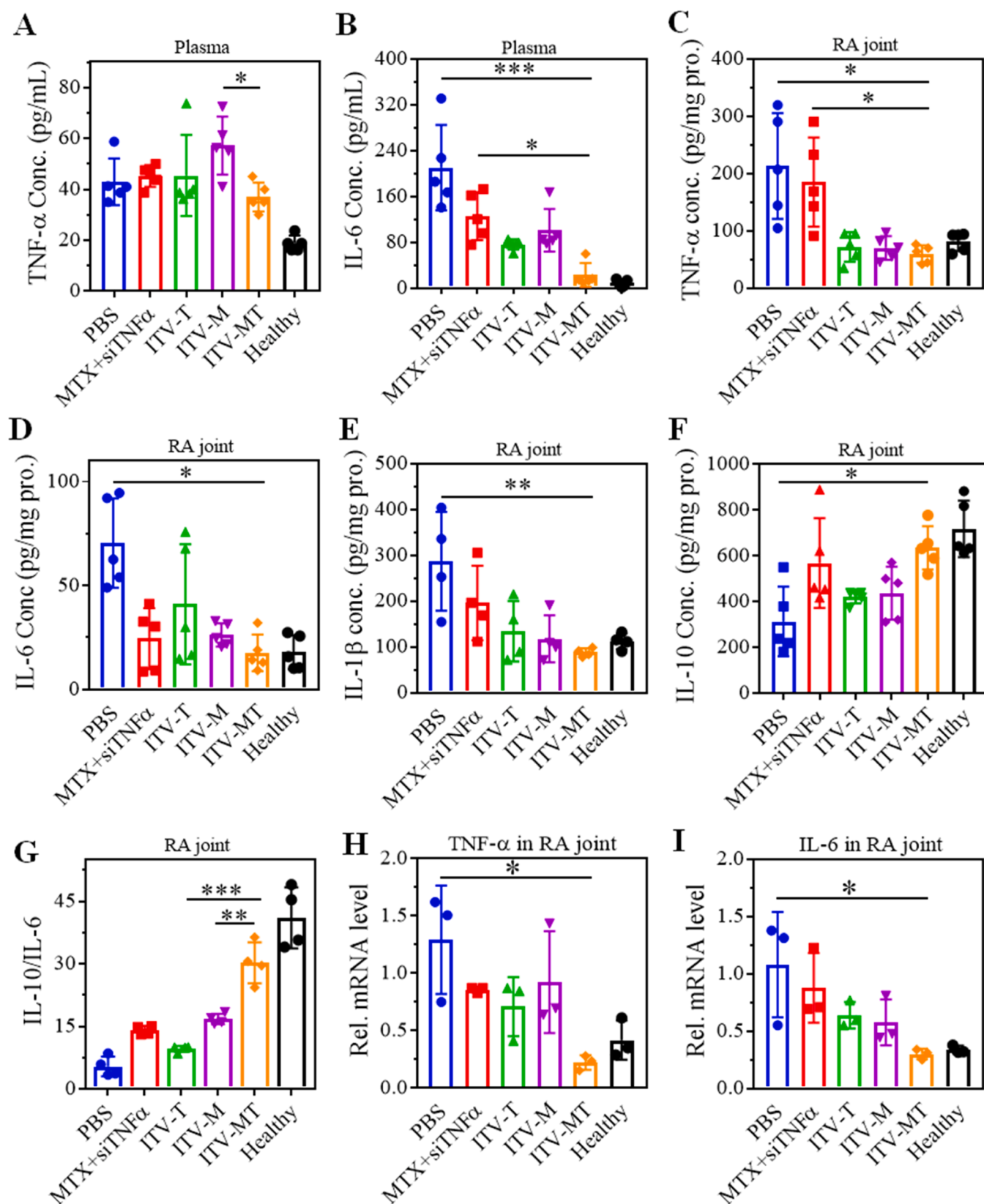


Fig. 5. Cytokine secretion and mRNA expression in CIA mice on day 16 after treatment, as shown in Fig. 4A. Concentrations of (A) TNF-α, (B) IL-6 in plasma, and (C) TNF-α ($n = 5$), (D) IL-6 ($n = 5$), (E) IL-1β ($n = 4$), (F) IL-10 ($n = 5$), and (G) ratio of IL-10/IL-6 ($n = 4$) in RA joints ($n = 5$). The expression of (H) TNF-α mRNA and (I) IL-6 mRNA in RA joints ($n = 3$).

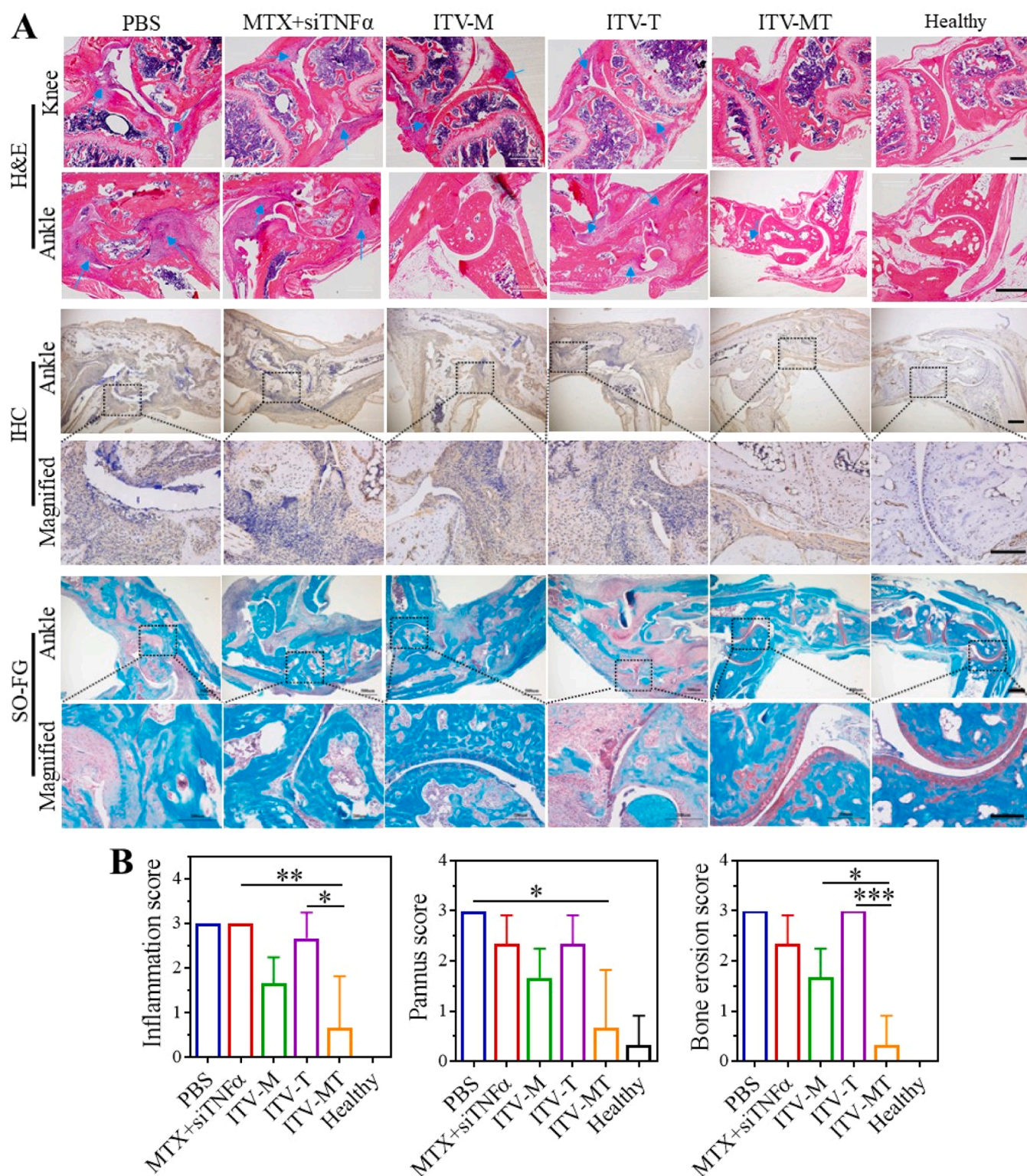


Fig. 6. Histological analysis of knee and ankle joints of the RA mice on day 16, as shown in Fig. 4A. (A) Representative H&E stained images, immunohistochemistry images of TNF- α and SO-FG stained images (scale bars: 200 μ m). Orange arrows in H&E images point to severe inflammation areas, white arrows in IHC images point to highly TNF- α positive areas, and red arrows in SO-FG images point to damaged synovial cartilage. (B) Semiquantitative scoring of synovial inflammation, pannus (from H&E staining) and bone erosion (from SO-FG staining) of CIA mice ($n = 3$).

more accurate model that reflects the RA patient scenario.

4. Conclusion

This study demonstrates that inflammation-targeted polymeric

vesicles codelivering MTX and siTNF α (ITV-MT) achieve synergistic efficacy in the ablation of CIA in mice. By combining a low dose of MTX with siTNF α to inhibit the TNF- α pathway, ITV-MT offers an effective therapeutic strategy for CIA mice that are insensitive to MTX monotherapy. ITV-MT exhibited robust co-loading capacities for MTX and

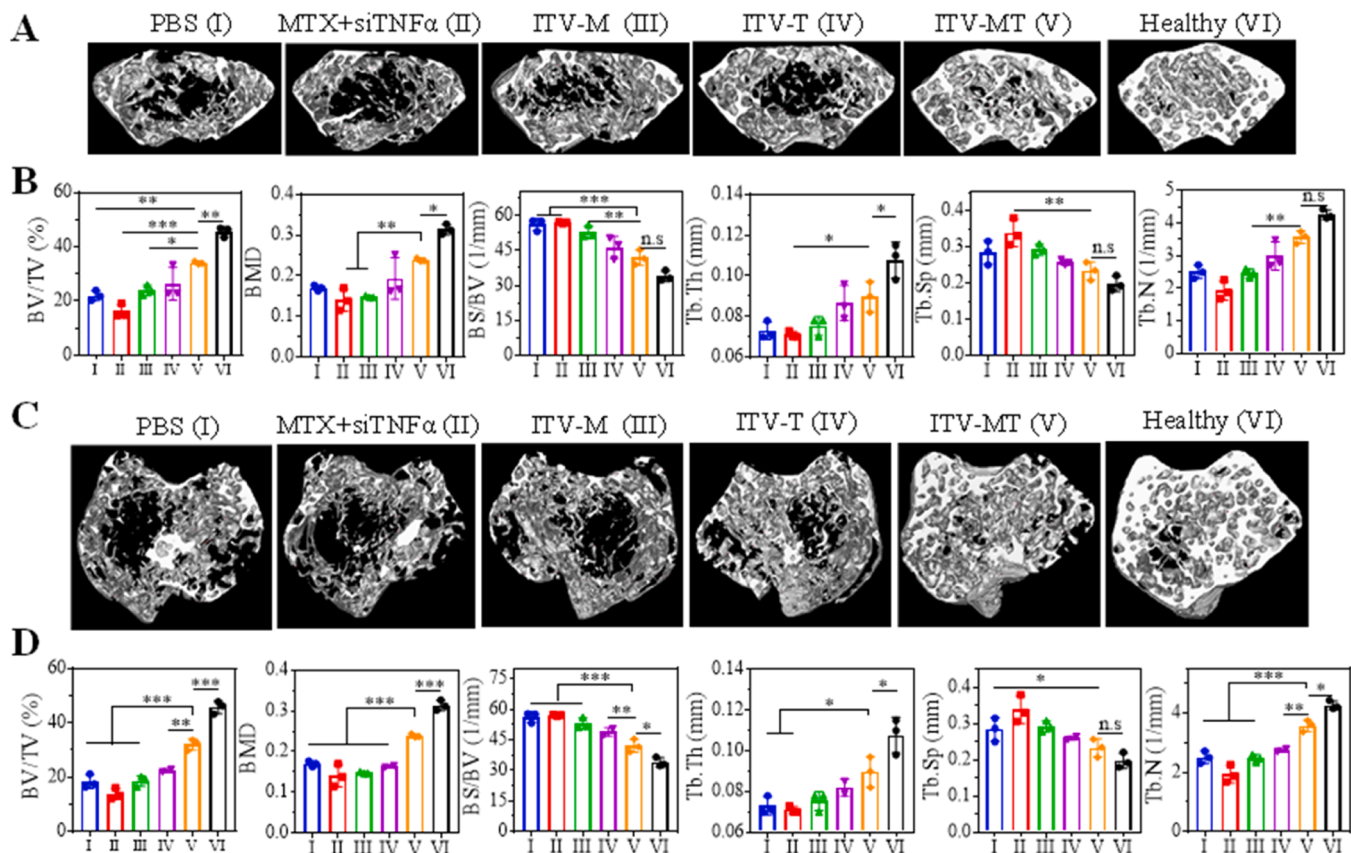


Fig. 7. Bone damage analysis of the tibias and femurs of CIA mice on day 16 after treatment, as shown in Fig. 4A ($n = 3$). (A) μ CT images of the cross-section and (B) structural parameters of the tibias. (C) μ CT images of the cross-section and (D) structural parameters of the femurs (bone volume fraction (BV/TV), bone mineral density (BMD), bone surface/volume ratio (BS/BV), trabecular thickness (Tb.Th), trabecular number (Tb.N), and trabecular separation (Tb.Sp)).

siTNF α , maintained a uniform size, and demonstrated efficient codelivery of both drugs to RA sites following intravenous injection in CIA mice. Notably, ITV-MT effectively downregulated proinflammatory cytokines while enhancing anti-inflammatory cytokine within the RA joints. This led to a substantial reduction in arthritis score and symptom relief compared to single drug-loaded polymersomes. Furthermore, ITV-MT effectively inhibited inflammatory cell infiltration in the RA synovium and protected against bone erosion and joint damage. This strategy leverages the synergistic effects of both drugs to modulate the inflammatory microenvironment. This inflammation-targeted codelivery of MTX and siTNF α provides a potential treatment strategy for RA patients and warrants further investigation.

CRediT authorship contribution statement

Liang Yang: Conceptualization, Data curation, Formal analysis, Investigation, Methodology, Writing – original draft. **Yongjie Sha:** Investigation, Data curation, Formal analysis. **Yuansong Wei:** Investigation, Formal analysis. **Lichen Yin:** Supervision, Resources. **Zhiyuan Zhong:** Supervision, Conceptualization, Writing – review & editing. **Fenghua Meng:** Conceptualization, Supervision, Funding acquisition, Project administration, Validation, Writing – review & editing.

Declaration of competing interest

The authors declare that they have no known competing financial interests or personal relationships that could have appeared to influence the work reported in this paper.

Acknowledgment

This work is supported by research grants from the National Natural Science Foundation of China (NSFC 52033006, 52473142).

Supplementary materials

Supplementary material associated with this article can be found, in the online version, at [doi:10.1016/j.actbio.2025.02.005](https://doi.org/10.1016/j.actbio.2025.02.005).

References

- [1] W. Zhang, Y. Chen, Q. Liu, M. Zhou, K. Wang, Y. Wang, J. Nie, S. Gui, D. Peng, Z. He, Z. Li, Emerging nanotherapeutics alleviating rheumatoid arthritis by readjusting the seeds and soils, *J. Control. Rel.* 345 (2022) 851–879.
- [2] Q. Xiao, X. Li, Y. Li, Z. Wu, C. Xu, Z. Chen, W. He, Biological drug and drug delivery-mediated immunotherapy, *Acta Pharm. Sin. B* 11 (4) (2021) 941–960.
- [3] A. Di Matteo, J.M. Bathon, P. Emery, Rheumatoid arthritis, *Lancet* 402 (10416) (2023) 2019–2033.
- [4] L. Zhang, Z. Qin, H. Sun, X. Chen, J. Dong, S. Shen, L. Zheng, N. Gu, Q. Jiang, Nanoenzyme engineered neutrophil-derived exosomes attenuate joint injury in advanced rheumatoid arthritis via regulating inflammatory environment, *Bioact. Mater.* 18 (2022) 1–14.
- [5] G. Nygaard, G.S. Firestein, Restoring synovial homeostasis in rheumatoid arthritis by targeting fibroblast-like synoviocytes, *Nat. Rev. Rheumatol.* 16 (6) (2020) 316–333.
- [6] Y. Yang, L. Guo, Z. Wang, P. Liu, X. Liu, J. Ding, W. Zhou, Targeted silver nanoparticles for rheumatoid arthritis therapy via macrophage apoptosis and repolarization, *Biomaterials* 264 (2021) 120390–120405.
- [7] R.B. Guo, X.Y. Zhang, D.K. Yan, Y.J. Yu, Y.J. Wang, H.X. Geng, Y.N. Wu, Y. Liu, L. Kong, X.T. Li, Folate-modified triptolide liposomes target activated macrophages for safe rheumatoid arthritis therapy, *Biomater. Sci.* 10 (2) (2022) 499–513.
- [8] P.E. Lipsky, D.M.F.M.v.d. Heijde, E.W.S. Clair, D.E. Furst, F.C. Breedveld, J. R. Kalden, J.S. Smolen, M. Weisman, P. Emery, M. Feldmann, G.R. Harriman, R. N. Maini, Infliximab and methotrexate in the treatment of rheumatoid arthritis, *N. Engl. J. Med.* 343 (22) (2000) 1594–1602.

- [9] B.N. Cronstein, T.M. Aune, Methotrexate and its mechanisms of action in inflammatory arthritis, *Nat. Rev. Rheumatol.* 16 (3) (2020) 145–154.
- [10] B.N. Cronstein, Low-dose methotrexate: a mainstay in the treatment of rheumatoid arthritis, *Pharmacol. Rev.* 57 (2) (2005) 163–172.
- [11] J.E. Gottenberg, J. Morel, E. Perrodeau, T. Bardin, B. Combe, M. Dougados, R. M. Flipo, A. Saraux, T. Schaevebeke, J. Sibilia, M. Soubrier, O. Vittecoq, G. Baron, A. Constantin, P. Ravaut, X. Mariette, R. French Society of, O.R.A. The investigators participating in Air, R. registries, comparative effectiveness of rituximab, abatacept, and tocilizumab in adults with rheumatoid arthritis and inadequate response to TNF inhibitors: prospective cohort study, *Brit. Med. J.* 364 (2019) l67.
- [12] M. Greenwood, M. Shipa, S.A. Yeoh, E. Roussou, D. Mukerjee, M.R. Ehrenstein, Methotrexate reduces withdrawal rates of TNF inhibitors due to ineffectiveness in rheumatoid arthritis but only in patients who are seropositive, *Ann. Rheum. Dis.* 79 (11) (2020) 1516–1517.
- [13] P.C. Taylor, Are TNF inhibitors still the agent of choice for RA? *Nat. Rev. Rheumatol.* 19 (12) (2023) 755–756.
- [14] G. Jezernik, M. Gorenjak, U. Potocnik, Gene ontology analysis highlights biological processes influencing non-response to anti-TNF therapy in rheumatoid arthritis, *Biomedicines* 10 (8) (2022) 1808.
- [15] J.S. Smolen, A.L. Pangan, P. Emery, W. Rigby, Y. Tanaka, J.I. Vargas, Y. Zhang, N. Damjanov, A. Friedman, A.A. Othman, H.S. Camp, S. Cohen, Upadacitinib as monotherapy in patients with active rheumatoid arthritis and inadequate response to methotrexate (SELECT-MONOTHERAPY): a randomised, placebo-controlled, double-blind phase 3 study, *Lancet* 393 (10188) (2019) 2303–2311.
- [16] J. Zhao, X. Zhang, X. Sun, M. Zhao, C. Yu, R.J. Lee, F. Sun, Y. Zhou, Y. Li, L. Teng, Dual-functional lipid polymeric hybrid pH-responsive nanoparticles decorated with cell penetrating peptide and folate for therapy against rheumatoid arthritis, *Eur. J. Pharm. Biopharm.* 130 (2018) 39–47.
- [17] A. Strangfeld, G.R. Burmester, Methotrexate: what are the true risks of treatment? *Ann. Rheum. Dis.* 79 (10) (2020) 1267–1268.
- [18] P. Wiland, A. Blauvelt, L. Lemke, O. Von Richter, A. Balfour, F. Furlan, N. Gaylis, Ab0208 Do low concentrations of citrate in an adalimumab formulation impact the incidence and/or intensity of injection site pain? Data from phase I and III studies assessing the local tolerance of Gp2017 (Adalimumab Biosimilar, Sdz-Adl) in healthy volunteers, rheumatoid arthritis, and psoriasis patients, *Ann. Rheum. Dis.* 80 (1) (2021) 1130–1131. Suppl.
- [19] N. Marasini, G. Er, C. Fu, C.N. Subasic, J. Ibrahim, M. Skwarczynski, I. Toth, A. K. Whittaker, L.M. Kaminskas, Development of a hyperbranched polymer-based methotrexate nanomedicine for rheumatoid arthritis, *Acta Biomater.* 142 (2022) 298–307.
- [20] L. Yang, Y. Sha, Y. Wei, H. Fang, J. Jiang, L. Yin, Z. Zhong, F. Meng, Mannose-mediated nanodelivery of methotrexate to macrophages augments rheumatoid arthritis therapy, *Biomater. Sci.* 11 (2023) 2211–2220.
- [21] H. Chen, Y. Sun, X. Xu, Q. Ye, Targeted delivery of methotrexate by modified yeast beta-glucan nanoparticles for rheumatoid arthritis therapy, *Carbohydr. Polym.* 284 (2022) 119183.
- [22] Y. Wang, Z. Liu, T. Li, L. Chen, J. Lyu, C. Li, Y. Lin, N. Hao, M. Zhou, Z. Zhong, Enhanced therapeutic effect of RGD-modified polymeric micelles loaded with low-dose methotrexate and nimesulide on rheumatoid arthritis, *Theranostics* 9 (3) (2019) 708–720.
- [23] M. Zhang, Y. Wen, Z. Huang, X. Qin, M. Zhou, D. Xiao, W. Cui, Z. Liu, Y. Lin, Targeted therapy for autoimmune diseases based on multifunctional frame nucleic acid system: blocking TNF- α -NF- κ B signaling and mediating macrophage polarization, *Chem. Eng. J.* 454 (2023) 140399.
- [24] N. Feng, F. Guo, Nanoparticle-siRNA: a potential strategy for rheumatoid arthritis therapy? *J. Control. Rel.* 325 (2020) 380–393.
- [25] V. Andretto, S. Dusi, S. Zilio, M. Repellino, D. Kryza, S. Ugel, G. Lollo, Tackling TNF- α in autoinflammatory disorders and autoimmune diseases: from conventional to cutting edge in biologics and RNA-based nanomedicines, *Adv. Drug Deliv. Rev.* 201 (2023) 115080.
- [26] S.J. Lee, A. Lee, S.R. Hwang, J.S. Park, J. Jang, M.S. Huh, D.G. Jo, S.Y. Yoon, Y. Byun, S.H. Kim, I.C. Kwon, I. Youn, K. Kim, TNF- α gene silencing using polymerized siRNA/thiolated glycol chitosan nanoparticles for rheumatoid arthritis, *Mol. Ther.* 22 (2) (2014) 397–408.
- [27] A.M. Aldayel, H.L. O'Mary, S.A. Valdes, X. Li, S.G. Thakkar, B.E. Mustafa, Z. Cui, Lipid nanoparticles with minimum burst release of TNF- α siRNA show strong activity against rheumatoid arthritis unresponsive to methotrexate, *J. Control. Rel.* 283 (2018) 280–289.
- [28] M.A.A. Jansen, L.H. Klausen, K. Thanki, J. Lyngso, J. Skov Pedersen, H. Franzyk, H. M. Nielsen, W. van Eden, M. Dong, F. Broere, C. Foged, X. Zeng, Lipidoid-polymer hybrid nanoparticles loaded with TNF siRNA suppress inflammation after intra-articular administration in a murine experimental arthritis model, *Eur. J. Pharm. Biopharm.* 142 (2019) 38–48.
- [29] M.F. Rai, H. Pan, H. Yan, L.J. Sandell, C.T.N. Pham, S.A. Wickline, Applications of RNA interference in the treatment of arthritis, *Transl. Res.* 214 (2019) 1–16.
- [30] C. Li, Y. Du, H. Lv, J. Zhang, P. Zhuang, W. Yang, Y. Zhang, J. Wang, W. Cui, W. Chen, Injectable amphiphatic artesunate prodrug-hydrogel microsphere as gene/drug nano-microplex for rheumatoid arthritis therapy, *Adv. Funct. Mater.* 32 (2022) 2206261.
- [31] Y. Li, S. Wei, Y. Sun, S. Zong, Y. Sui, Nanomedicine-based combination of dexamethasone palmitate and MCL-1 siRNA for synergistic therapeutic efficacy against rheumatoid arthritis, *Drug Deliv. Transl. Res.* 11 (6) (2021) 2520–2529.
- [32] J. Li, L. Chen, X. Xu, Y. Fan, X. Xue, M. Shen, X. Shi, Targeted combination of antioxidative and anti-inflammatory therapy of rheumatoid arthritis using multifunctional dendrimer-entrapped gold nanoparticles as a platform, *Small* 16 (49) (2020) e2005661.
- [33] N. Yin, X. Tan, H. Liu, F. He, N. Ding, J. Gou, T. Yin, H. He, Y. Zhang, X. Tang, A novel indomethacin/methotrexate/MMP-9 siRNA in situ hydrogel with dual effects of anti-inflammatory activity and reversal of cartilage disruption for the synergistic treatment of rheumatoid arthritis, *Nanoscale* 12 (15) (2020) 8546–8562.
- [34] S. Nasra, D. Bhatia, A. Kumar, Targeted macrophage re-programming: synergistic therapy with methotrexate and RELA siRNA folate-liposome in RAW264.7 cells and arthritic rats, *Adv. Healthc. Mater.* 13 (22) (2024) 2400679.
- [35] K. Uehara, T. Harumoto, A. Makino, Y. Koda, J. Iwano, Y. Suzuki, M. Tanigawa, H. Iwai, K. Asano, K. Kurihara, A. Hamaguchi, H. Kodaira, T. Atsumi, Y. Yamada, K. Tomizuka, Targeted delivery to macrophages and dendritic cells by chemically modified mannose ligand-conjugated siRNA, *Nucleic Acids Res.* 50 (9) (2022) 4840–4859.
- [36] E.A. Ross, A. Devitt, J.R. Johnson, Macrophages: the good, the bad, and the gluttony, *Front. Immunol.* 12 (2021) 708186.
- [37] L. Liu, F. Hu, H. Wang, X. Wu, A.S. Eltahan, S. Stanford, N. Bottini, H. Xiao, M. Bottini, W. Guo, X.J. Liang, Secreted protein acidic and rich in cysteine mediated biomimetic delivery of methotrexate by albumin-based nanomedicines for rheumatoid arthritis therapy, *ACS Nano* 13 (5) (2019) 5036–5048.
- [38] Y.J. Yang, L.J. Lu, J.J. Wang, S.Y. Ma, B.L. Xu, R. Lin, Q.S. Chen, Z.G. Ma, Y.L. Mo, D.T. Wang, Tubson-2 decoction ameliorates rheumatoid arthritis complicated with osteoporosis in CIA rats involving isochlorogenic acid A regulating IL-17/MAPK pathway, *Phytomedicine* 116 (2023) 154875.
- [39] Y. Zou, J. Wei, Y. Xia, F. Meng, J. Yuan, Z. Zhong, Targeted chemotherapy for subcutaneous and orthotopic non-small cell lung tumors with cyclic RGD-functionalized and disulfide-crosslinked polymersomal doxorubicin, *Signal Transduct. Target. Ther.* 3 (1) (2018) 32.
- [40] S. Cecioni, A. Imberty, S. Vidal, Glycomimetics versus multivalent glycoconjugates for the design of high affinity lectin ligands, *Chem. Rev.* 115 (1) (2015) 525–561.
- [41] N. Varga, I. Sutkeviciute, C. Guzzi, J. McGeagh, I. Petit-Haertlein, S. Gugliotta, J. Weiser, J. Angulo, F. Fieschi, A. Bernardi, Selective targeting of dendritic cell-specific intercellular adhesion molecule-3 grabbing nonintegrin (DC-SIGN) with mannose-based glycomimetics: synthesis and interaction studies of bis (benzylamide) derivatives of a pseudomannobioside, *Chem. Eur. J.* 19 (15) (2013) 4786–4797.
- [42] T. Ganbold, H. Baigude, Design of mannose-functionalized curdlan nanoparticles for macrophage-targeted siRNA delivery, *ACS Appl. Mater.* 10 (17) (2018) 14463–14474.
- [43] B.E. Collins, J.C. Paulson, Cell surface biology mediated by low affinity multivalent protein-glycan interactions, *Curr. Opin. Chem. Biol.* 8 (6) (2004) 617–625.
- [44] K. Kannan, R.A. Ortmann, D. Kimpel, Animal models of rheumatoid arthritis and their relevance to human disease, *Pathophysiology* 12 (3) (2005) 167–181.
- [45] L. Bevaart, M.J. Vervordeldonk, P.P. Tak, Evaluation of therapeutic targets in animal models of arthritis: how does it relate to rheumatoid arthritis? *Arthritis Rheum.* 62 (8) (2010) 2192–2205.
- [46] Y. Zhao, V. Urbonaviciute, B. Xu, W. Cai, Z. Sener, C. Ge, R. Holmdahl, Cartilage oligomeric matrix protein induced arthritis—A new model for rheumatoid arthritis in the C57BL/6 mouse, *Front. Immunol.* 12 (2021) 631249.
- [47] E. van Mulligen, A. van der Helm-van Mil, P.H.P. de Jong, Methotrexate prolongs TNF inhibitor survival, but only in autoantibody-positive rheumatoid arthritis: a validation study, *Ann. Rheum. Dis.* 82 (10) (2023) e217.
- [48] Z. Zhao, Z. Hua, X. Luo, Y. Li, L. Yu, M. Li, C. Lu, T. Zhao, Y. Liu, Application and pharmacological mechanism of methotrexate in rheumatoid arthritis, *Biomed. Pharmacother.* 150 (2022) 113074.
- [49] N. Pishesha, T. Harmand, L.Y. Smeding, W. Ma, L.S. Ludwig, R. Janssen, A. Islam, Y.J. Xie, T. Fang, N. McCaul, W. Pinney, H.R. Sugito, M.A. Rossotti, G. Gonzalez-Sapientza, H.L. Ploegh, Induction of antigen-specific tolerance by nanobody-antigen adducts that target class-II major histocompatibility complexes, *Nat. Biomed. Eng.* 5 (11) (2021) 1389–1401.
- [50] R.D. Bell, M. Brendel, M.A. Konnaris, L.B. Ivashkiv, F. Wang, Automated multi-scale computational pathotyping (AMSCP) of inflamed synovial tissue, *Nat. Commun.* 15 (1) (2024) 7503.
- [51] K. Kachler, D. Andreev, S. Thapa, D. Royzman, A. Gieß, S. Karuppusamy, M. L. Perez, M. Liu, J. Hofmann, A. Gessner, X. Meng, S. Rauber, A. Steinkasserer, M. Fromm, G. Schett, A. Bozec, Aco1-mediated inhibition of aerobic glycolysis suppresses osteoclast differentiation and attenuates bone erosion in arthritis, *Ann. Rheum. Dis.* 83 (12) (2024) 1691.